

Chiral edge plasmons in quantum anomalous Hall insulators

Furu Zhang,^{1,2,*} Chenxi Ding,^{3,4,*} Jianhui Zhou,^{3,†} and Yugui Yao^{2,‡}

¹*School of Science, Beijing Forestry University, Beijing 100083, China*

²*Key Laboratory of Advanced Optoelectronic Quantum Architecture and Measurement (MOE), School of Physics, Beijing Institute of Technology, Beijing 100081, China*

³*Anhui Key Laboratory of Low-Energy Quantum Materials and Devices, High Magnetic Field Laboratory, HFIPS, Anhui, Chinese Academy of Sciences, Hefei 230031, P. R. China*

⁴*University of Science and Technology of China, Hefei, 230026, P. R. China*

We find that the Berry curvature splits the edge plasmons propagating along the opposite directions in quantum anomalous Hall insulators even with vanishing Chern number. When the bulk is insulating, only one unidirectional edge plasmon mode survives whose direction can be changed by external fields. The unidirectional edge plasmon in the long-wavelength limit is acoustic and essentially determined by the anomalous Hall conductivity. The group velocity of the chiral edge plasmon would change its sign for a large wave vector, which originates from the k -quadratic correction to the effective mass. The impacts of the Fermi level and the wave vector on the bulk and edge plasmons are discussed. Our work provides a well quantitative explanation of the recent observation of the chiral edge plasmon in quantum anomalous Hall insulators and some insight into the application of realistic topological materials in chiral plasmonics.

Introduction.--Berry phase is a key ingredient of modern quantum theory and plays an important role in the development of topological phases of matter and topological materials [1]. Recently, the Berry phase effect on the plasmon excitations in solids has attracted increasing attentions [2–11]. Several theoretical works have shown that the Berry curvature, an effective magnetic field in momentum space, should split the energy spectra of edge plasmons in the metallic systems such as photo-excited two-dimensional (2D) gapped Dirac materials at zero external magnetic fields [4, 5]. Unlike the conventional magnetoplasmons [12–16], magnetic fields are not need to break the time reversal symmetry and to rise a definite chirality of magnetoplasmons. In addition, the chiral plasmons induced by the Berry curvature are themselves handed and essentially differ from those ones in either metallic handed nanoparticles or handed groupings of individual resonant nanoparticles for chiral plasmonics [17].

Topological materials including topological insulators (TIs) [18, 19] and topological semimetals [20] provide us promising platforms to investigate the impacts of the topology of the Bloch bands on collective excitations [21, 22]. Recently there have been a series of important experimental progress on plasmon excitations in the topological materials [23–32]. In particular, the contactless microwave circulator response suggests the existence of the chiral edge plasmons in magnetized disks of TIs, Cr-doped $(\text{Bi}, \text{Sb})_2\text{Te}_3$, that support the quantum anomalous Hall effect (QAHE) [33–35]. These chiral edge plasmons exhibit a strong magnetic-free nonreciprocity that enables us to design and implement nonreciprocal devices in photonics [36] and transceiver technology [37–39]. Unlike the conventional band insulators, the QAH insulators host robust chiral edge states [40–45], which may support the chiral edge plasmons. However, a thor-

ough and direct theoretical explanation of the chiral edge plasmons in QAH insulators as well as their manipulation remain unexplored.

In this work, we show that the Berry curvature splits the energy dispersion of edge plasmons in the magnetically doped thin films of TIs. When the bulk is insulating, only one unidirectional edge plasmon mode survives, whose direction can be changed by external fields. The unidirectional edge plasmon in the long-wavelength limit is acoustic and entirely determined by the quantum anomalous Hall conductivity and the effective dielectric constant of the environment. For a large wave vector, the group velocity of the chiral edge plasmon would change its sign, which originates from the k -quadratic correction of the effective mass. The behaviors of both the bulk and edge plasmons dependent on the Fermi level and the wave vector are discussed.

Formalism of edge plasmons.--We begin with a physical model of the system, in which a 2D semi-infinite QAH system occupying the region $x < 0$ is put on

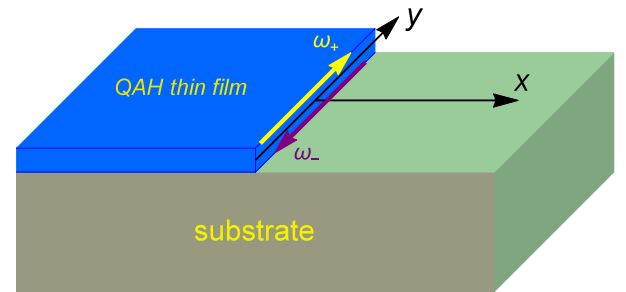


Figure 1. A schematic drawing of the physical model of edge plasmons ω_{\pm} near the edge between the QAH insulator and a vacuum. The 2D semi-infinite QAH system is put on the substrate, occupying the region $x < 0$.

the substrate, as shown in Fig. 1. The effective dielectric constant of the substrate ($z < 0$) is ϵ_{sub} , and there is a vacuum for $z > 0$. We consider an edge along the y direction. The edge plasmon excitations are governed by a set of self-consistent equations [46]: the Poisson's equation $\nabla \cdot [\epsilon E(\mathbf{r})] = \rho(x, y)\delta(z)$, and the equation of continuity $\nabla \cdot \mathbf{j}(x, y) = i\omega\rho(x, y)$, where $\rho(x, y) = \rho(x)e^{i(qy - \omega t)}$ is the charge density fluctuation and $\mathbf{j}_\alpha(x, y) = \sum_\beta \sigma_{\alpha\beta} E_\beta(x, y, z = 0)$ is the current den-

sity. The frequency and wave vector dependent electrical conductivity tensor $\sigma_{\alpha\beta}(q, \omega)$ is calculated through the general Kubo formula [47]. $\epsilon = \epsilon_0$ for $z > 0$ and $\epsilon = \epsilon_{sub}\epsilon_0$ for $z < 0$. In this work, we use the average surrounding dielectric constant $\epsilon = (1 + \epsilon_{sub})\epsilon_0/2 = 7\epsilon_0$ to directly compare with the recent experiment, in which the QAH insulator is grown on the substrate of semi-insulating GaAs [33].

The dispersion relations of plasmons can be obtained from solving the set of self-consistent equations above. By means of the Laguerre series [46, 48], one gets the numerical solutions in a matrix equation:

$$\det[J_{mn} + (\eta_1 \pm \chi)I_m - \delta_{mn}] = 0, \quad (1)$$

where the parameters are $\eta_1 = \frac{|q|\sigma_{xx}}{i\epsilon\omega}$, $\eta_2 = \frac{|q|\sigma_{yy}}{i\epsilon\omega}$ and $\chi = \frac{|q|\sigma_{xy}}{\epsilon\omega}$. We leave the specific expressions of J_{mn} and I_m given in the Supplemental Material [49].

After choosing the approximate expression of the integral kernel [12, 13], one can analytically solve the self-consistent equations and yield the corresponding dispersion relation of the edge plasmons [49]

$$\eta_1\eta_2 - 2\eta_1 - \eta_2 - \chi^2 \pm 2\sqrt{2}\chi = 0, \quad (2)$$

where the plus (minus) sign denotes that the edge plasmon propagates along the y ($-y$) direction. From Eq. (2), one clearly sees that a non-zero transverse conductivity or anomalous Hall conductivity σ_{xy} breaks the degeneracy of the edge plasmons propagating in opposite directions, yielding a pair of chiral plasmons. For the time reversal invariant system, the anomalous Hall conductivity σ_{xy} should vanish. Thus the two edge plasmon modes are degenerate. Note that taking $\eta_1 = \eta_2$, Eq. (2) would reduce to the counterpart for the edge magnetoplasmons in 2D electron gases [50, 51].

Chiral plasmons in doped QAH insulators.--Let us consider the behaviors of plasmons near the edge of the QAH insulators. To demonstrate the main physics, we choose the effective model for QAH insulators in magnetically doped thin films of three-dimensional strong TIs V- and Cr-doped (Bi, Sb)₂Te₃ [6, 52]:

$$H = H_0 + \frac{m}{2}\tau_0 \otimes \sigma_z, \quad (3)$$

where m is the exchange field originating from the magnetic dopants, effectively acting as a Zeeman field. H_0 is

given as [53]

$$H_0 = -Dk^2 + \begin{pmatrix} h_+(\mathbf{k}) & V \\ V & h_-(\mathbf{k}) \end{pmatrix}, \quad (4)$$

with

$$h_\pm(\mathbf{k}) = \begin{pmatrix} \pm(\frac{\Delta}{2} - Bk^2) & iv_F k_- \\ -iv_F k_+ & \mp(\frac{\Delta}{2} - Bk^2) \end{pmatrix}, \quad (5)$$

where $h_\pm(\mathbf{k})$ describes the 2D Dirac fermions with a k -dependent mass. $\mathbf{k} = (k_x, k_y)$ is the 2D wave vector and $k_\pm = k_x \pm ik_y$. v_F is the effective velocity. The D term breaks the particle-hole symmetry and splits the longitudinal bulk plasmon modes [6]. Δ is the hybridization of the top and bottom surface states of the thin film. V measures the structural inversion asymmetry between the top and bottom surfaces. Pauli matrices τ_0 and σ_z act on the pseudospin space related to the top and bottom surfaces and the real spin degree of freedom, respectively. Here we primarily consider the insulating phase that requires $|D| < |B|$. In addition, we take the parameters in real calculations such that the theoretical calculations of energy bands are in a good agreement with experimental observations [41, 42]. Specifically, $v_F = 3.0 \text{ eV} \cdot \text{\AA}$, $\Delta = -0.01 \text{ eV}$ and $B = -30 \text{ eV} \cdot \text{\AA}^2$.

By the numerical solutions to Eq. (1) and the approximate analytical results from Eq. (2), we obtain the plasmon dispersions in doped QAH insulators in both the topologically trivial ($\xi \equiv -m/m_0 < 1$ with $m_0 = \sqrt{4V^2 + \Delta^2}$) and nontrivial ($\xi > 1$) phases, as plotted in Fig. 2. The plasmon modes possess several key features. First, there are two edge plasmon modes propagating in opposite directions near the edge for both the topological nontrivial (Fig. 2(a)) and trivial (Fig. 2(b)) phases. It is a sharp contrast to the previous theoretical work on metallic systems that requires a nonzero anomalous Hall conductivity or mean Berry curvature to split the edge plasmon into a pair of chiral edge plasmons [4, 5, 54]. We define the mode propagating along the y direction as ω_+ , and the opposite mode as ω_- . Second, Fig. 2 shows that the two edge plasmons are not degenerate and the energy of mode ω_+ is higher than mode ω_- . Third, the numerical results are well consistent with the corresponding approximate analytical solutions, and the energy of the former is slightly higher [55]. Fourth, in contrast to the conventional magnetoplasmons in the context of 2D electron gases [12, 13, 46], both of the two edge plasmons are gapless. When the wave vector q is small, ω_+ and ω_- are nearly degenerate. As the wave vector q increases, the split of the two edge plasmon modes becomes pronounced. The energy of the edge plasmons is lower than the bulk plasmon that is determined by the zeros of the complex dielectric function $\epsilon(q, \omega)$ [6], *i.e.* $\omega_{bulk} > \omega_+ > \omega_-$. In the direction perpendicular to the edge of the material, mode ω_- decays faster than ω_+ . For a sufficiently large wave vector q , the fast mode ω_+

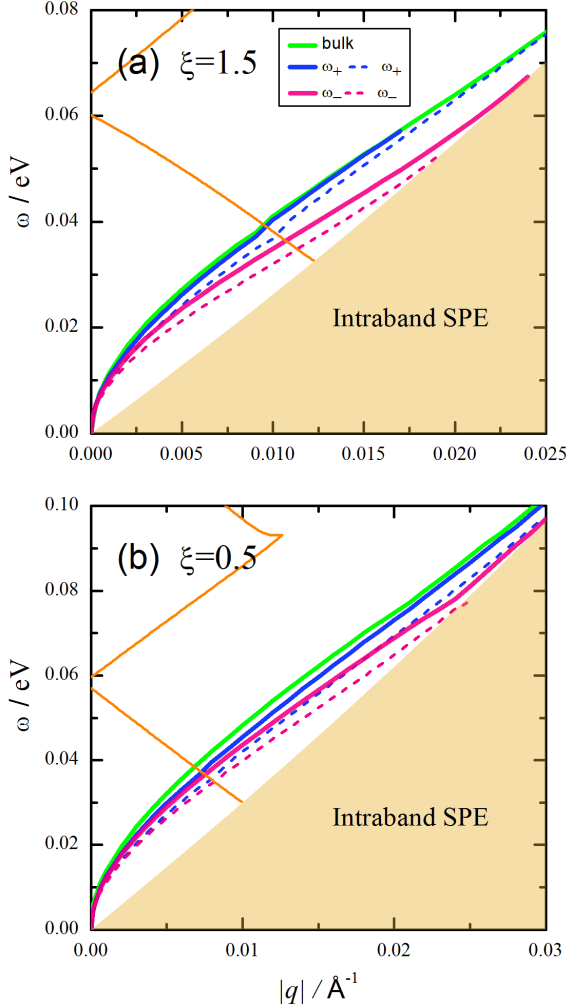


Figure 2. The bulk plasmon (green lines) and chiral edge plasmons (blue and purple lines) of semi-infinite QAH insulators in different topological phases: $\xi = 1.5$ for a nontrivial phase with a unit Chern number in (a) and $\xi = 0.5$ for a trivial phase with a vanishing Chern number in (b). The orange lines refer to the boundary of the interband SPEs. The solid (dashed) line indicates the numerical exact (approximate) solutions. The parameters are $\mu = 0.09$ eV and $V = 0.03$ eV, $D = 10$ eV \AA^2 .

will merge with bulk mode ω_{bulk} . Consequently, only the edge plasmon ω_- survives along the edge until it enters into the intraband single-particle excitations (SPEs) region. In fact, the interband SPEs have little influence on the plasmons because of tiny overlap of energy bands for the frequency range we discussed here. In addition, comparing Figs. 2(a) with 2(b), the behavior of the chiral plasmons in different phases are similar, while the energy splitting of ω_{\pm} in the nontrivial phase is much bigger than those in the trivial phase.

Unidirectional plasmons in intrinsic systems.—When the bulk is insulating, the bulk plasmon ω_{bulk} will disappear due to lack of free bulk electrons at the Fermi

level. But the edge plasmon still exists and is unidirectional. From the perspective of semiclassical dynamics, the Berry curvature $\Omega(\mathbf{k})$ acts as an effective magnetic field in momentum space and modifies the kinematic equation of electrons with an anomalous velocity $-\frac{e}{h}\mathbf{E} \times \Omega(\mathbf{k})$, which essentially accounts for various anomalous transport and optical properties of Bloch electrons in solids [1]. The sign of the Berry curvature determines the direction of the anomalous velocity then significantly affects the behaviors of edge plasmons. Specifically, for a nonzero wave vector q , there exists a single unidirectional edge plasmon propagating on the edge of the magnetically doped TIs, even when it is topologically trivial.

We solve the matrix equation in Eq. (1) in the undoped case and plot the dispersion curves of the edge plasmons in Figs. 3(a)-3(d) [56]. When $m < 0$, both Eq. (1) and Eq. (2) have only one solution, in which the wave vector q is positive. So the edge plasmon is an unidirectional mode and propagates in the positive direction, *i.e.* ω_+ . If $m > 0$, the sign of Berry curvature changes and the unidirectional edge plasmon will accordingly become mode ω_- . This salient character agrees with the recent experiment about magnetoplasmons in a QAH insulator [33]. In their experiment, the frequency of the edge plasmon is about GHz, which is marked in the insert of Fig. 3(b). Our numerical results show that the velocity of the edge plasmon is about 2.93 eV \cdot \AA and well consistent with the experimental data 2.63 eV \cdot \AA [33]. Figure 3(c) shows the dependence of energy dispersions of the chiral plasmons on the exchange field m for $\mu = 0$ eV and $\mu = 0.02$ eV. For the Fermi level in the band gap, the frequency of chiral plasmons is independent on the magnitude of exchange fields, which is well consistent with the experimental result [33]. On the contrary, the frequency of chiral plasmons strongly depends on the magnitude of magnetization for the lightly doped case.

In the long-wavelength limit $q \rightarrow 0$, we have $\sigma_{xx} \approx \sigma_{yy} \approx 0$, and $\sigma_{xy} \approx \pm e^2/h$ for the nontrivial phase (h is Planck's constant and e the electron charge). Inserting σ_{xy} into Eq. (2), one immediately gets the dispersion relation of the edge plasmon:

$$\omega_{H+}(q) = \frac{q\sigma_{xy}}{2\sqrt{2}\epsilon} = \frac{|q|}{2\sqrt{2}\epsilon} \frac{e^2}{h}. \quad (6)$$

It is clear that such edge plasmon is an acoustic mode whose velocity is solely determined by the quantum Hall conductivity e^2/h and the effective dielectric constant of the environment, but independent of the detailed parameters of the system. The corresponding velocity of the edge plasmon in the long-wavelength limit is about 1.46 eV \cdot \AA and much less than the experimental value [57]. This is a unique collective mode appearing only in the QAH insulators. The numerical solutions share the same character, as shown in Fig. 3(a). When the system is in a nontrivial phase ($\xi > 1$), all the dispersion curves

of the edge plasmons approach the same asymptotic line in the long-wavelength limit. While for a trivial phase ($\xi < 1$), the dispersion curves tend to zero. Thus, the dispersion properties of the unidirectional edge plasmon strongly depends on the topology of the system. In sum, our work could reproduce all key features of the chiral edge plasmons in the QAH insulator. It is one of the central results in this work.

Origin of negative dispersion.--Figure 3(d) shows that, when the wave vector q is large enough, the dispersion starts to bend downward such that the group velocity of the edge plasmons could become negative. It happens in both the topologically trivial and nontrivial phases. In the rest of this section, we would like to reveal the mechanism for the negative dispersion of edge plasmons.

For simplicity, we assume $V = 0$ and $D = 0$, the effective Hamiltonian in Eq. (3) reduces to two diagonalized blocks with replacing $\Delta/2$ with $M_{\pm} = (m \pm \Delta)/2$ in $h_{\pm}(\mathbf{k})$. When $B = 0$, the Hamiltonian above describes 2D massive Dirac fermions with mass of M_{\pm} . By use of the Kubo formula, one can calculate the transverse conductivity in the intrinsic case ($\omega > 0$) [49]

$$\sigma_{xy}(q, \omega) = \frac{e^2}{h} \sum_{a=\pm} \frac{M_a}{\sqrt{v_F^2 q^2 - \omega^2}} \left(\arctan \frac{2|M_a|}{\sqrt{v_F^2 q^2 - \omega^2}} - \frac{\pi}{2} \right), \quad (7)$$

where the exchange field m gives rise to a non-zero transverse conductivity. In the limit $q \rightarrow \infty$, we have

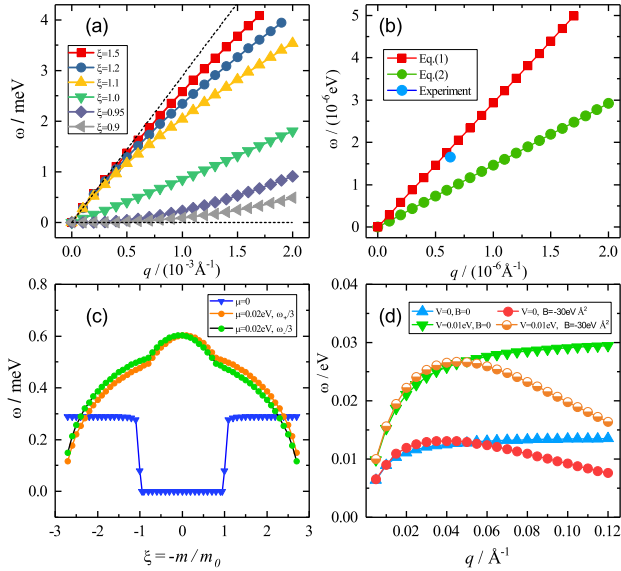


Figure 3. (a) Energy dispersion of the unidirectional edge plasmon for selected values of ξ . (b) The theoretical dispersions of the chiral edge plasmon in the long-wavelength limit is in accordance with the experimental results in Ref. [33]. (c) The dependence of frequency of the chiral edge plasmon with $q = 10^{-4}/\text{\AA}$ on ξ for different chemical potentials. (d) The velocity of the edge plasmon in topologically nontrivial phase with $\xi = 1.5$ becomes negative for a sufficiently large wave vector q . The parameters are $D = 0$, and $V = 0.01 \text{ eV}$.

$\sigma_{xy} = -e^2 m \pi / 2 \hbar v_F |q|$. Consequently, from Eq. (2) one get a single unidirectional edge plasmon, whose energy is independent of q : $\omega_{H+} = \frac{e^2 |m| \pi}{4 \sqrt{2} \hbar e v_F}$. For $V \neq 0$, this is also true suggested by the numerical results (seen in Fig. 3(d)). Thus, for a large enough wave vector q , the dispersion curve of the unidirectional edge plasmon (green and blue lines) becomes a flat band, and no negative dispersion appears in the system.

When $v_F = 0$, Eq. (5) reduces to a model for the conventional 2D semiconductors. Accordingly, the integrand in the Kubo formula becomes an odd function of k_x , and then one gets $\sigma_{xy}(q, \omega) = 0$. As a result, ω_+ vanishes. More generally, this is true even in the situation that $V \neq 0$ and $D \neq 0$ so long as there is no term like k_x^n in the Hamiltonian where n is an odd number. Thus, there is even no edge plasmons in the conventional 2D semiconductors with a vanishing σ_{xy} .

One thus finds that the negative dispersion of edge plasmons requires the coexistence of the linear and quadratic terms of k . It is entirely different from the previous mechanisms [47, 58, 59]. In this situation, $\omega \propto q \sigma_{xy}$ is still satisfied but the quadratic term Bk^2 will change the behavior of the transverse conductivity. In the limit $q \rightarrow \infty$, our numerical calculation implies that $\sigma_{xy} \propto |q|^{-\alpha}$ with $\alpha \approx 4$. As a result, the group velocity of the edge plasmon (red and orange lines) becomes negative, as shown in Fig. 3(d).

Manipulation of chiral plasmons.--It has been demonstrated that the transverse conductivity $\sigma_{xy}(q, \omega)$ plays a crucial role in forming the chiral plasmons [60]. Thus, one could manipulate the chiral edge plasmons including the number and the direction of the modes by tuning $\sigma_{xy}(q, \omega)$ in experiments. Specifically, the tunable Fermi level through the gate voltage, ionic liquid or doping [61] could change $\sigma_{xy}(q, \omega)$ even its sign. For instance, for the n -doped case, the bigger the Fermi energy μ , the smaller $\sigma_{xy}(q, \omega)$. As a result, the energy split of the chiral plasmons $\Delta\omega \equiv \omega_+ - \omega_-$ will decrease. On the other hand, higher Fermi energy can also increase the gap between ω_{bulk} and ω_+ , preventing ω_+ from merging with the bulk mode.

Figure 4 depicts the behaviors of the bulk and chiral edge plasmons versus the wave vector q and the Fermi energy μ . For a larger enough Fermi energy μ , the edge plasmons ω_{\pm} and the bulk plasmon ω_{bulk} coexist. As μ decreases, ω_+ mode becomes delocalized along the direction perpendicular to the edge and gradually merges with the bulk plasmon. Then the ω_- mode and the bulk mode ω_{bulk} will enter the intra-band SPE region successively and are damped, leaving no plasmon excitations. Note that this always happens for a general wave vector. It is worth pointing out that when the Fermi level lies in the band gap, there exists only one single edge-plasmon mode ω_{H+} , which is dominated by the transverse conductivity. Meanwhile, when the system is lightly doped,

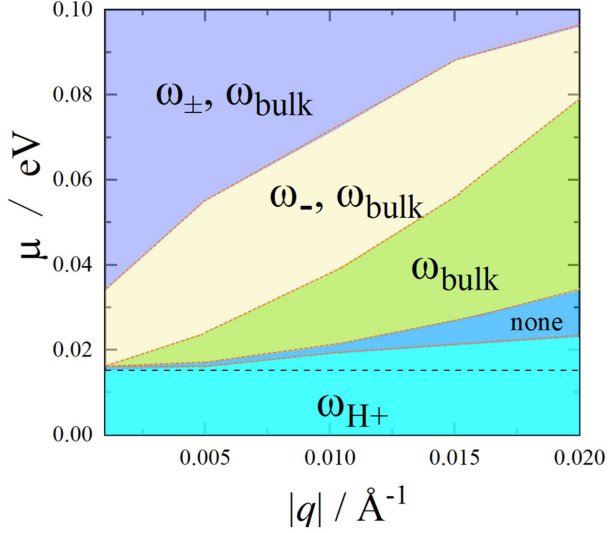


Figure 4. Dependence of the bulk and edge plasmons on the Fermi energy and the wave vector. The horizontal dashed line indicates the magnitude of band gap. Parameters are identical to those in Fig. 2(a).

ω_{H+} can also survive until the longitudinal conductivity becomes comparable to the transverse one.

In summary, we showed that the Berry curvature splits the degeneracy of edge plasmons, leading to the chiral plasmons in the QAH insulators. When the system enters into the QAH phase, only one unidirectional edge plasmon survives, whose propagation direction can be flipped by the external magnetization. In the long-wavelength limit, the unidirectional edge plasmon is acoustic and entirely determined by the anomalous Hall conductivity and the effective dielectric constant. We provide a quantitative explanation of the recent observation of the chiral edge plasmons in QAH insulators and find the negative dispersion of chiral edge plasmon and reveal its unusual physical origin. Therefore, our work could be applicable to the tunable intrinsic magnetic topological materials hosting QAHE, such as MnBi_2Te_4 [62–65].

This work was supported by the National Key R&D Program of China (Grant No. 2020YFA0308800) and by the National Natural Science Foundation of China (No. 12174394). J.Z. was supported by the HFIPS Director's Fund (Grant Nos. YZJJQY202304 and BJPY2023B05) and Chinese Academy of Sciences under contract No. JZHKYPT-2021-08 and also by the High Magnetic Field Laboratory of Anhui Province.

* These authors contributed equally to this work.

† jhzhou@hmf.ac.cn

‡ ygyao@bit.edu.cn

[1] D. Xiao, M. C. Chang, and Q. Niu,

- Rev. Mod. Phys. **82**, 1959 (2010).
- [2] S. Juergens, P. Michetti, and B. Trauzettel, Phys. Rev. Lett. **112**, 076804 (2014).
- [3] J. Zhou, H.-R. Chang, and D. Xiao, Phys. Rev. B **91**, 035114 (2015).
- [4] A. Kumar, A. Nemilentsau, K. H. Fung, G. Hanson, N. X. Fang, and T. Low, Phys. Rev. B **93**, 041413 (2016).
- [5] J. C. W. Song and M. S. Rudner, Proceedings of the National Academy of Sciences **113**, 4658 (2016).
- [6] F. Zhang, J. Zhou, D. Xiao, and Y. Yao, Phys. Rev. Lett. **119**, 266804 (2017).
- [7] S. S.-L. Zhang and G. Vignale, Phys. Rev. B **97**, 224408 (2018).
- [8] J. Cao, H. A. Fertig, and L. Brey, Phys. Rev. Lett. **127**, 196403 (2021).
- [9] S. F. Islam and A. A. Zyuzin, Phys. Rev. B **104**, 245301 (2021).
- [10] S. Heidari, D. Culcer, and R. Asgari, Phys. Rev. B **103**, 035306 (2021).
- [11] Z. Liang and T. Liu, Phys. Rev. B **107**, 224426 (2023).
- [12] A. L. Fetter, Phys. Rev. B **32**, 7676 (1985).
- [13] A. L. Fetter, Phys. Rev. B **33**, 3717 (1986).
- [14] V. A. Volkov and S. A. Mikhailov, Sov. Phys. JETP **67**, 1639 (1988).
- [15] H. Bartolomei, R. Bisognin, H. Kamata, J.-M. Berroir, E. Bocquillon, G. Ménard, B. Plaçais, A. Cavanna, U. Gennser, Y. Jin, P. Degiovanni, C. Mora, and G. Fève, Phys. Rev. Lett. **130**, 106201 (2023).
- [16] A. A. Sokolik and Y. E. Lozovik, Phys. Rev. B **109**, 165430 (2024).
- [17] M. Hentschel, M. Schäferling, X. Duan, H. Giessen, and N. Liu, Science Advances **3**, e1602735 (2017).
- [18] M. Z. Hasan and C. L. Kane, Rev. Mod. Phys. **82**, 3045 (2010).
- [19] X.-L. Qi and S.-C. Zhang, Rev. Mod. Phys. **83**, 1057 (2011).
- [20] N. P. Armitage, E. J. Mele, and A. Vishwanath, Rev. Mod. Phys. **90**, 015001 (2018).
- [21] S. Maier, *Plasmonics: Fundamentals and Applications* (Springer US, 2010).
- [22] A. Grigorenko, M. Polini, and K. Novoselov, Nature photonics **6**, 749 (2012).
- [23] P. Di Pietro, M. Ortolani, O. Limaj, A. Di Gaspere, V. Giliberti, F. Giorgianni, M. Brahlek, N. Bansal, N. Koirala, S. Oh, *et al.*, Nat. Nanotechnol. **8**, 556 (2013).
- [24] J.-Y. Ou, J.-K. So, G. Adamo, A. Sulaev, L. Wang, and N. I. Zheludev, Nat. Commun. **5** (2014).
- [25] A. Kogar, S. Vig, A. Thaler, M. H. Wong, Y. Xiao, D. Reig-i Plessis, G. Y. Cho, T. Valla, Z. Pan, J. Schneeloch, R. Zhong, G. D. Gu, T. L. Hughes, G. J. MacDougall, T.-C. Chiang, and P. Abbamonte, Phys. Rev. Lett. **115**, 257402 (2015).
- [26] Y. D. Glinka, S. Babakiray, T. A. Johnson, M. B. Holcomb, and D. Lederman, Nat. Commun. **7**, 13054 (2016).
- [27] X. Jia, S. Zhang, R. Sankar, F.-C. Chou, W. Wang, K. Kempa, E. W. Plummer, J. Zhang, X. Zhu, and J. Guo, Phys. Rev. Lett. **119**, 136805 (2017).
- [28] A. Politano, G. Chiarello, B. Ghosh, K. Sadhukhan, C.-N. Kuo, C. S. Lue, V. Pellegrini, and A. Agarwal, Phys. Rev. Lett. **121**, 086804 (2018).
- [29] S. Xue, M. Wang, Y. Li, S. Zhang, X. Jia, J. Zhou, Y. Shi, X. Zhu, Y. Yao, and J. Guo, Phys. Rev. Lett. **127**, 186802 (2021).

- [30] C. Wang, Y. Sun, S. Huang, Q. Xing, G. Zhang, C. Song, F. Wang, Y. Xie, Y. Lei, Z. Sun, and H. Yan, *Phys. Rev. Appl.* **15**, 014010 (2021).
- [31] Y. Shao, A. J. Sternbach, B. S. Y. Kim, A. A. Rikhter, X. Xu, U. D. Giovannini, R. Jing, S. H. Chae, Z. Sun, S. H. Lee, Y. Zhu, Z. Mao, J. C. Hone, R. Queiroz, A. J. Millis, P. J. Schuck, A. Rubio, M. M. Fogler, and D. N. Basov, *Science Advances* **8**, eadd6169 (2022).
- [32] Y. Li, M. Wang, Y. Li, S. Xue, J. Li, Z. Tao, X. Han, J. Zhou, Y. Shi, J. Guo, and X. Zhu, *Phys. Rev. B* **107**, 155421 (2023).
- [33] A. C. Mahoney, J. I. Colless, L. Peeters, S. J. Pauka, E. J. Fox, X. Kou, L. Pan, K. L. Wang, D. Goldhaber-Gordon, and D. J. Reilly, *Nat. Commun.* **8**, 1836 (2017).
- [34] T. Wang, C. Wu, M. Mogi, M. Kawamura, Y. Tokura, Z.-X. Shen, Y.-Z. You, and M. T. Allen, *Phys. Rev. B* **108**, 235432 (2023).
- [35] L. A. Martinez, G. Qiu, P. Deng, P. Zhang, K. G. Ray, L. Tai, M.-T. Wei, H. He, K. L. Wang, J. L. DuBois, and D.-X. Qu, *Phys. Rev. Res.* **6**, 013081 (2024).
- [36] L. Feng, M. Ayache, J. Huang, Y.-L. Xu, M.-H. Lu, Y.-F. Chen, Y. Fainman, and A. Scherer, *Science* **333**, 729 (2011).
- [37] L. Bi, J. Hu, P. Jiang, D. H. Kim, G. F. Dionne, L. C. Kimerling, and C. A. Ross, *Nature Photonics* **5**, 758 (2011).
- [38] N. A. Estep, D. L. Sounas, J. Soric, and A. Alù, *Nature Physics* **10**, 923 (2014).
- [39] A. C. Mahoney, J. I. Colless, S. J. Pauka, J. M. Hornibrook, J. D. Watson, G. C. Gardner, M. J. Manfra, A. C. Doherty, and D. J. Reilly, *Phys. Rev. X* **7**, 011007 (2017).
- [40] F. D. M. Haldane, *Phys. Rev. Lett.* **61**, 2015 (1988).
- [41] R. Yu, W. Zhang, H.-J. Zhang, S.-C. Zhang, X. Dai, and Z. Fang, *Science* **329**, 61 (2010).
- [42] C.-Z. Chang, J. Zhang, X. Feng, J. Shen, Z. Zhang, M. Guo, K. Li, Y. Ou, P. Wei, L.-L. Wang, *et al.*, *Science* **340**, 167 (2013).
- [43] A. J. Bestwick, E. J. Fox, X. Kou, L. Pan, K. L. Wang, and D. Goldhaber-Gordon, *Phys. Rev. Lett.* **114**, 187201 (2015).
- [44] H. Weng, R. Yu, X. Hu, X. Dai, and Z. Fang, *Advances in Physics* **64**, 227 (2015).
- [45] C.-Z. Chang, C.-X. Liu, and A. H. MacDonald, *Rev. Mod. Phys.* **95**, 011002 (2023).
- [46] J.-W. Wu, P. Hawrylak, G. Eliasson, and J. J. Quinn, *Phys. Rev. B* **33**, 7091 (1986).
- [47] G. Giuliani and G. Vignale, *Quantum theory of the electron liquid* (Cambridge University Press, Cambridge, UK, 2005).
- [48] W. Wang, P. Apell, and J. Kinet, *Phys. Rev. B* **84**, 085423 (2011).
- [49] See Supplemental Material for the derivations of main formulas in the main text, which includes Refs. [52, 53, 66].
- [50] D. B. Mast, A. J. Dahm, and A. L. Fetter, *Phys. Rev. Lett.* **54**, 1706 (1985).
- [51] J. W. Wu, P. Hawrylak, and J. J. Quinn, *Phys. Rev. Lett.* **55**, 879 (1985).
- [52] H.-Z. Lu, A. Zhao, and S.-Q. Shen, *Phys. Rev. Lett.* **111**, 146802 (2013).
- [53] H. Zhang, C.-X. Liu, X.-L. Qi, X. Dai, Z. Fang, and S.-C. Zhang, *Nature physics* **5**, 438 (2009).
- [54] Y. Zhang, F. Zhai, B. Guo, L. Yi, and W. Jiang, *Phys. Rev. B* **96**, 045104 (2017).
- [55] W. Wang, J. M. Kinet, and S. P. Apell, *Phys. Rev. B* **85**, 235444 (2012).
- [56] By solving the matrix equation of Eq. (1) in the intrinsic case, we choose a smooth boundary condition (see details in Supplemental Material [49]), whose electric current has the form $j_x(x \geq 0) = j_x(x = 0^-)e^{-\kappa x}$ where $\kappa \gg |q|$ is used to avoid divergence of the plasmon frequency in the long-wavelength limit.
- [57] The discrepancy between theoretical values of the velocity of the chiral edge plasmon through the numerical and approximate methods and the experimental result might originate from the treatment of the density profile of electrons near the edge of the QAH insulator.
- [58] F. Aryasetiawan and K. Karlsson, *Phys. Rev. Lett.* **73**, 1679 (1994).
- [59] J. van Wezel, R. Schuster, A. König, M. Knupfer, J. van den Brink, H. Berger, and B. Büchner, *Phys. Rev. Lett.* **107**, 176404 (2011).
- [60] X. Lin, Z. Liu, T. Stauber, G. Gómez-Santos, F. Gao, H. Chen, B. Zhang, and T. Low, *Phys. Rev. Lett.* **125**, 077401 (2020).
- [61] G. Zheng, M. Wang, X. Zhu, C. Tan, J. Wang, S. Albarakati, N. Aloufi, M. Algarni, L. Farrar, M. Wu, Y. Yao, M. Tian, J. Zhou, and L. Wang, *Nature Communications* **12**, 3639 (2021).
- [62] Y. Gong, J. Guo, J. Li, K. Zhu, M. Liao, X. Liu, Q. Zhang, L. Gu, L. Tang, X. Feng, D. Zhang, W. Li, C. Song, L. Wang, P. Yu, X. Chen, Y. Wang, H. Yao, W. Duan, Y. Xu, S.-C. Zhang, X. Ma, Q.-K. Xue, and K. He, *Chinese Physics Letters* **36**, 076801 (2019).
- [63] Y. Deng, Y. Yu, M. Z. Shi, Z. Guo, Z. Xu, J. Wang, X. H. Chen, and Y. Zhang, *Science* **367**, 895 (2020).
- [64] R. Mei, Y.-F. Zhao, C. Wang, Y. Ren, D. Xiao, C.-Z. Chang, and C.-X. Liu, *Phys. Rev. Lett.* **132**, 066604 (2024).
- [65] S. K. Chong, C. Lei, Y. Cheng, S. H. Lee, Z. Mao, A. H. MacDonald, and K. L. Wang, *Phys. Rev. Lett.* **132**, 146601 (2024).
- [66] S.-Q. Shen, *Topological Insulators: Dirac Equation in Condensed Matters*, Vol. 174 (Springer Science & Business Media, 2013).

This figure "fig4.png" is available in "png" format from:

<http://arxiv.org/ps/2404.13930v1>